Heavy quasiparticles formed in the ferromagnetic Yb layers in the Kondo helical magnet $YbNi_3Al_9$ as revealed by specific-heat measurements

Ryoichi Miyazaki,* Yuji Aoki,† Ryuji Higashinaka, and Hideyuki Sato
Department of Physics, Tokyo Metropolitan University, Hachioji, Tokyo 192-0397, Japan

Testuro Yamashita and Shigeo Ohara
Department of Engineering Physics, Electronics and Mechanics, Graduate School of Engineering, Nagoya Institute of Technology, Nagoya 466-8555, Japan
(Received 26 July 2012; published 2 October 2012)

We report specific-heat and magnetocaloric-effect studies on single-crystalline Kondo helical magnet $YbNi_3Al_9$. Molecular field analysis of a Schottky peak due to the Zeeman splitting of the Yb-ion doublet crystalline-field ground state demonstrates that the interlayer antiferromagnetic exchange interactions are 2 orders of magnitude smaller than that of the intralayer ferromagnetic coupling among Yb ions, reflecting realization of magnetically well separated Yb layers. The Sommerfeld coefficient γ, which is 110 mJ/K^2 mol in zero field, decreases smoothly with increasing field without any noticeable anomalies at the helical magnetic phase boundary. This fact confirms that heavy quasiparticles are formed on a part of the Fermi surface away from "hot sheets" that have nesting instabilities responsible for the helical magnetic structure. These results indicate that $YbNi_3Al_9$ is a novel system where heavy quasiparticles are confined within the two-dimensional Yb layers.

DOI: 10.1103/PhysRevB.86.155106 PACS number(s): 75.30.Mb, 75.30.Kz, 75.40.Cx, 75.47.De

I. INTRODUCTION

Strongly correlated electron systems associated with f electrons have rich variety of ground states including the heavy-fermion (HF) state, unconventional superconductivity, multipolar ordering, and several types of quantum critical behaviors.[1–4] Many of them studied so far are three-dimensional (3D) types. Since the electron-electron correlation effect is expected to be significantly enhanced if interacting electrons are confined into lower dimensions, it is important to search for such low-dimensional f-electron systems. One approach reported recently is to produce artificial multilayers.[5,6] In $CeIn_3/LaIn_3$ and $CeCoIn_5/YbCoIn_5$ multilayers, suppression of a magnetic ordering ending up with a HF state and dimensionality tuning of superconductivity have been realized, respectively. In such systems, however, bulk properties including specific heat and magnetization are extremely difficult to be measured. Therefore, to search for "natural" low-dimensional f electron bulk materials is desired.

Here we report one candidate material $YbNi_3Al_9$, in which heavy quasiparticles are most probably confined in two-dimensional (2D) Yb layers. This compound crystallizes in the trigonal $ErNi_3Al_9$-type structure with the space group $R32$ (D_3^7, no. 155)[7,8] (see Fig. 1). Yb ions form a 2D honeycomb lattice in Yb_2Al_3 layers which stack along the c axis with a distance of $d_L = c/3 = 9.121$ Å. In between, seven triangular lattice layers of Al or Ni with the sequence of Al-Ni-Al-Al-Al-Ni-Al intervene. In the 2D honeycomb lattice, the nearest-neighbor Yb-Yb distance is $d_{n.n.} = a/\sqrt{3} = 4.199$ Å; i.e., $d_L/d_{n.n.} = 2.17$. Note that this value of $d_L/d_{n.n.}$ is much larger than 1.63 of the typical quasi-2D material $CeCoIn_5$ ($d_L = 7.56$ Å and $d_{n.n.} = 4.62$ Å).[9,10]

Reflecting the 2D nature of the crystal structure, $YbNi_3Al_9$ shows strongly anisotropic magnetic and transport properties. A helical magnetic (HM) ordering sets in at $T_{HM} = 3.4$ K.[11,12] The Yb magnetic moments are aligned ferromagnetically in the Yb_2Al_3 layers and rotate around the c axis with the propagation vector $\boldsymbol{q} = 0.8 \times \boldsymbol{c}^*$, which has been determined by a neutron-scattering experiment.[13] Below T_{HM}, the magnetization (M) curve shows a metamagnetic jump up to 1.2 μ_B at $H_M \simeq 0.1$ T at 2 K for $\boldsymbol{H} \parallel a$, while it increases gradually for $\boldsymbol{H} \parallel c$ ($M = 0.04$ μ_B at $\mu_0 H = 0.1$ T).[11] Strong correlations in the conduction electrons are inferred from the $-\log T$ dependence of resistivity above ~40 K, which is attributable to the Kondo effect in the Yb crystalline-electric-field (CEF)-split levels.[11,12] Below T_{HM}, the electronic specific-heat coefficient γ in zero field is 110 mJ/K^2 mol, providing thermodynamic evidence for quasiparticle mass enhancement.

In this paper, we report on low-temperature specific-heat and magnetocaloric effect (MCE) measurements of single-crystalline $YbNi_3Al_9$ in applied fields. The results indicate that heavy quasiparticles are confined within the 2D Yb layers.

II. EXPERIMENTAL DETAILS

A single crystal of $YbNi_3Al_9$ with a dimension of 5 × 5 × 3 mm^3 grown by the Al self-flux method using raw materials of 3N (99.9% pure)-Yb, 4N-Ni, and 5N-Al has been used for the present study (see Ref. 11 for more details about the sample preparation). Strong de Haas–van Alphen (dHvA) signals obtained from similarly prepared single crystals attest to their high quality.[14] Specific heat $C(H,T)$ has been measured by a quasiadiabatic heat-pulse method using a dilution refrigerator equipped with an 8-T superconducting magnet. The magnetic field is always applied along the a axis, i.e., parallel to the Yb 2D honeycomb lattice plane. With the same setup, MCE measurements have been performed by monitoring the variation of the sample temperature with sweeping the magnetic field between 0 and 0.3 T with a rate of 0.015 T/min. Magnetization measurements have been made using a commercial superconducting quantum interference device (SQUID) magnetometer MPMS (Quantum Design).

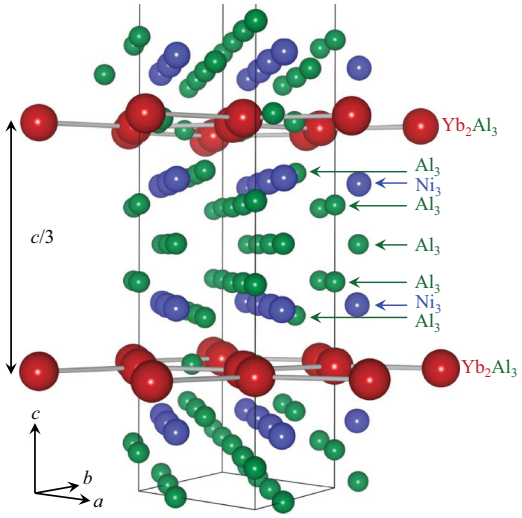

FIG. 1. (Color online) A part of the crystal structure of $YbNi_3Al_9$. See text for details.

III. RESULTS

Figure 2 shows specific heat divided by temperature C/T measured with $H \parallel a$. A clear λ-type anomaly appearing at $T_{HM} = 3.41$ K in $\mu_0 H = 0$ T corresponds to the helical magnetic ordering.[13] This value of T_{HM} is slightly higher than 3 K, which has been reported previously.[15] With increasing H, as shown in the inset, the peak initially shifts to lower temperatures for $\mu_0 H < 0.15$ T, reflecting the antiferromagnetic nature of the ordered phase. At $\mu_0 H = 0.075$ T, the peak height shows a maximum. Above 0.15 T, the peak becomes broader and shifts to higher temperatures with increasing H.

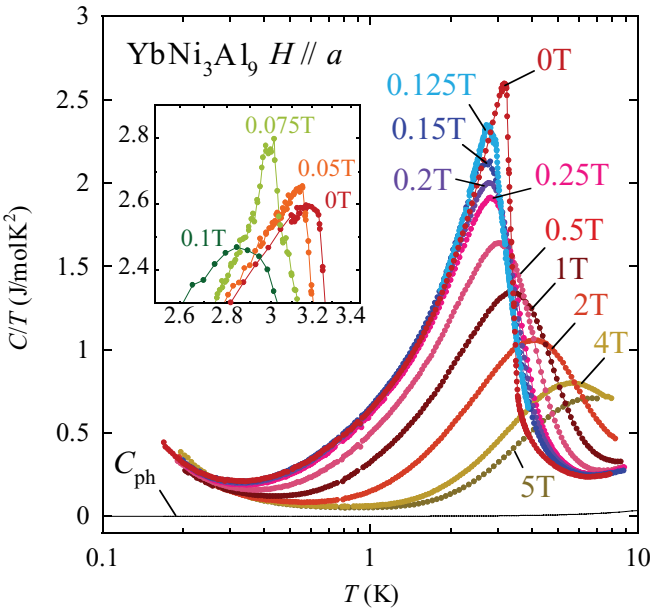

FIG. 2. (Color online) Temperature dependence of C/T measured in applied fields. An expanded view around the helical phase transition for $\mu_0 H \leqslant 0.1$ T is shown in the inset. The thin line represents the phonon part C_{ph} estimated from the specific-heat data of $LuNi_3Al_9$.

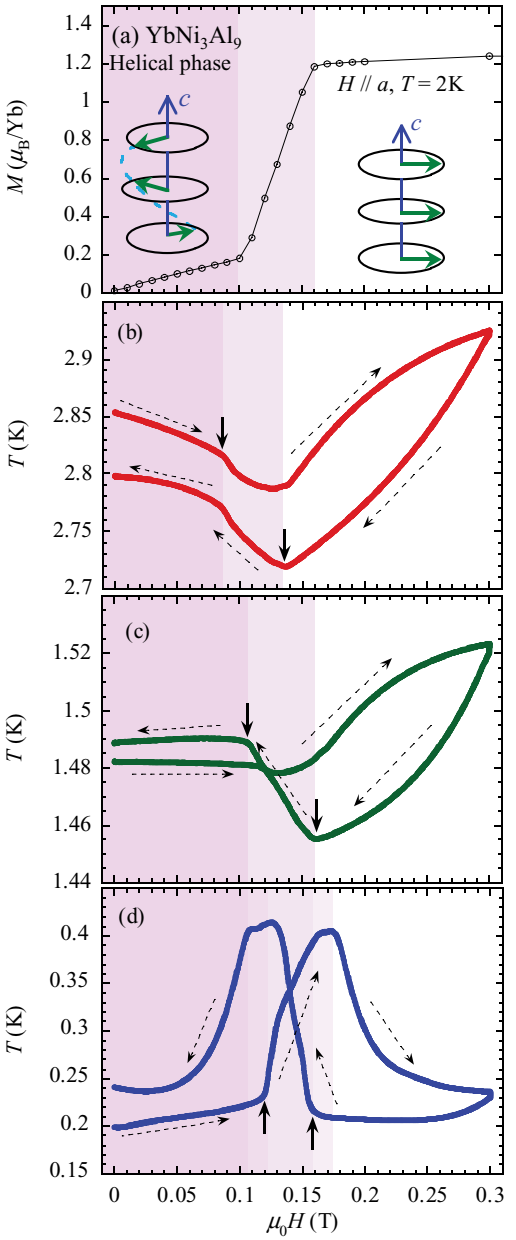

FIG. 3. (Color online) (a) Isothermal magnetization curves measured at 2 K. (b)–(d) T-vs-H curves of the magnetocaloric effect (MCE) measurements with $H \parallel a$. Solid arrows show the onsets of the metamagnetic transition and dashed lines with an arrow show the H sweeping directions.

It is clear from the comparison with the M-H curve shown in Fig. 3(a) that the metamagnetic anomaly appears at the boundary of the helical magnetic phase and it corresponds to a sharp peak in C/T for $\mu_0 H < 0.15$ T. At low temperatures, it is difficult to detect the phase boundary by specific-heat measurements, since the boundary runs parallel to the T axis in the H-vs-T space. Therefore, we have performed MCE measurements to detect the phase boundary.

Representative T-vs-H curves of the MCE measurements are displayed in Figs. 3(b)–3(d). For $T \sim 2.8$ K ($<T_{HM}$), irreversible contributions appearing in the T-vs-H curve is rather small, indicating that the sample is roughly in an adiabatic

condition (isentropic process), i.e., the thermodynamic relation $(dS/dH)_T = -(C_H/T)(dT/dH)_S$ holds approximately. $dT/dH < 0$ in the helical phase and $dT/dH > 0$ in the ferromagnetically polarized phase. In $0.09 < \mu_0 H < 0.13$ T, where the metamagnetic anomaly appears, dT/dH has larger negative values. With decreasing temperature, the irreversible heating contribution becomes pronounced, especially in the H regions where the metamagnetic anomaly appears. For $T \sim 1.5$ K, the heating contribution masks the intrinsic cooling behavior in the H increasing process, while it cooperatively enhances the intrinsic heating behavior in the H decreasing process. For $T \sim 0.2$ K, the irreversible heating at the metamagnetic transition (probably due to magnetic domain wall motion) becomes more dominant; the heating behavior appears in both sweeping processes and the intrinsic behavior of the isentropic process is no longer visible. From the H shift of the heating region between H increasing and decreasing processes, we infer that the hysteretic behavior of the order of ~0.02 T appears in the metamagnetic transition at 0.2 K.

From these results, the helical phase boundary in the H-T phase diagram has been determined as shown in Fig. 4(a). The critical field H_M at $T = 0$ K is estimated to be 0.14 T.

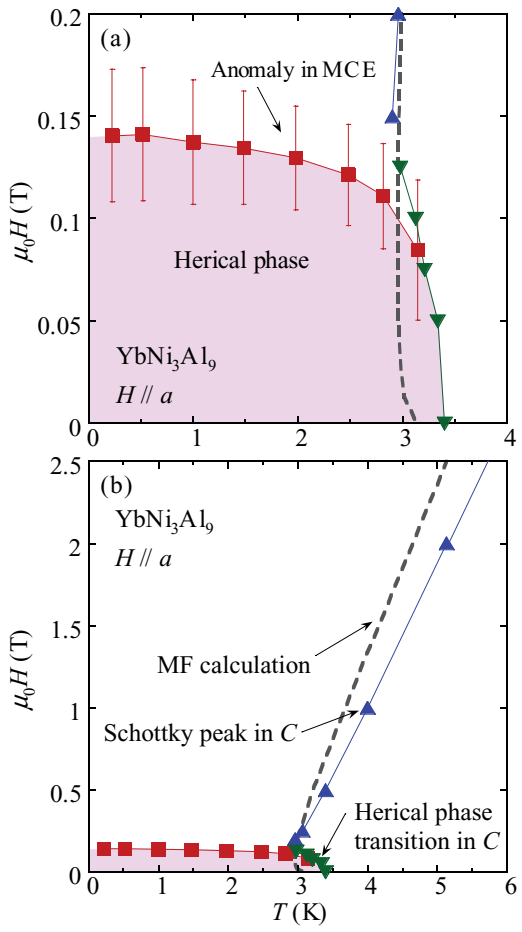

FIG. 4. (Color online) H-T phase diagram for low fields (a) and high fields (b) determined by specific-heat measurements (▲: Schottky peak in the FM phase, ▼: helical phase transition) and MCE (■). Dashed line shows a MF model calculation for the specific-heat peak position $T_p(H)$ (see text).

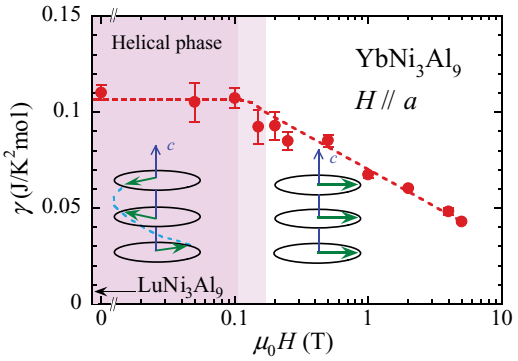

FIG. 5. (Color online) H dependence of γ. The dashed line is a guide to the eye.[16]

IV. DISCUSSION

In the measured temperature range, C of $YbNi_3Al_9$ has contributions from electrons ($C_{el} = \gamma T + C_{4f}$), phonons ($C_{ph} = \beta T^3$), and nuclear spins ($C_{nuc} = A/T^2$). Measured specific heat of $LuNi_3Al_9$ can be well expressed as $C = \gamma_{Lu} T + \beta_{Lu} T^3$, with $\gamma_{Lu} = 6.4$ mJ/K^2 mol and $\beta_{Lu} = 0.35$ mJ/K^4 mol at low temperatures.[11] We tentatively use β_{Lu} for β of $YbNi_3Al_9$. C_{ph} has only a minor contribution to the total C in $T < 10$ K, as shown in Fig. 2 by a thin solid line. C_{nuc} appears as an upturn below ~0.4 K for all H data. C_{4f}, representing contributions from $4f$ electrons of the Yb ions, can be phenomenologically expressed as $BT^n \exp(-\Delta/T)$ at low T below ~2 K.[16] The $C(T)$ data in $T \lesssim 2$ K have been fitted by a sum of these terms and the H dependence of γ is obtained as displayed in Fig. 5. In zero field, $\gamma = 110$ mJ/K^2 mol $\simeq 17\gamma_{Lu}$. This fact indicates that the quasiparticle mass is significantly enhanced even in the helical magnetic state. Note that γ decreases gradually with increasing H without showing any noticeable anomalies across the phase boundary of the helical magnetic state, indicating that the mass enhancement mechanism is not directly associated with the HM ordering or HM fluctuations.

Using the determined values of $A(H)$, $C_{el}(T,H)$ data have been obtained. The electronic entropy S_{el} calculated using the $C_{el}(T,H)$ data is shown in Fig. 6. S_{el} is 4.2 J/K^2 mol at $T = T_{HM}$ and reaches $R \ln 2$ at ~8.5 K. This is consistent with the fact that the valence of Yb ions is almost 3+,[17,18] and the $J = 7/2$ multiplet of the Yb ions splits into four doublets due to the CEF effect (the site symmetry of the $6c$ site is C_3) and the magnetic behaviors in $T < 10$ K are dominated by the CEF ground-state doublet. The entropy released above T_{HM}, i.e., $R \ln 2 - S_{el}(T_{HM})$, is attributable to the Kondo effect ($T_K \gtrsim 3$ K)[11] and/or the magnetic short-range ordering (ferromagnetic in the layers and helical between the layers).

In the field-induced ferromagnetic (FM) phase ($H > H_M$), the peak in C/T becomes broader and shifts to higher temperatures with increasing H, as shown in Fig. 2. This peak results from the Schottky-type thermal excitations between the two Zeeman-split energy levels of the CEF ground-state doublet; excitations to the first excited CEF level can only be seen above 7 K as a slight increase in C in zero field. The peak height C_{peak} shown in Fig. 7 is much higher than 3.65 J/K mol, which is expected for a doublet with a fixed energy separation, and depends on H significantly. This

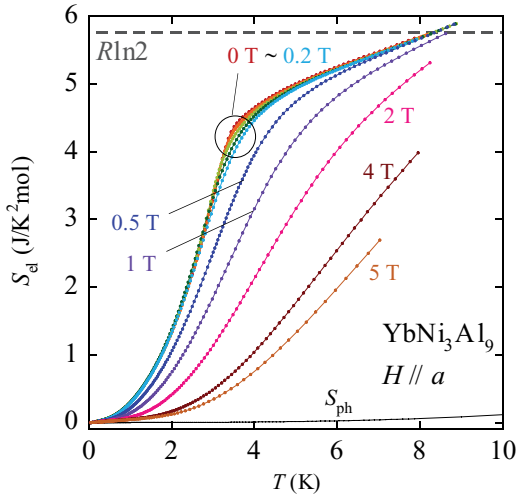

FIG. 6. (Color online) The temperature dependence of the electronic entropy S_{el}. For comparison, the lattice contribution S_{ph} is drawn by a thin line.

behavior indicates pronounced ferromagnetic interactions among Yb ions.

In the paramagnetic (PM) or field-induced FM phase, we analyze the $C(T,H)$ data taking into account the ferromagnetic interactions in a mean-field (MF) approximation. In our model, the Hamiltonian can be expressed as

$$\mathcal{H} = -g\mu_B s(H + \lambda g\mu_B \bar{s}) + \tfrac{1}{2}\lambda(g\mu_B\bar{s})^2, \qquad (1)$$

where a Yb magnetic moment is represented by $g\mu_B s$ using an in-plane pseudospin s ($\bar{s}$: thermal average), effective g factor, and the Bohr magneton μ_B. The MF coefficient λ is described as $\lambda = 2J_{FM}/(g\mu_B)^2$ using the exchange integral J_{FM}. When T is decreased, $\bar{s}(T,H)$ shows a significant development at a certain T range depending on the applied H. Because the energy separation of the CEF ground-state doublet ($\propto H + \lambda g\mu_B\bar{s}$) develops accordingly, this behavior

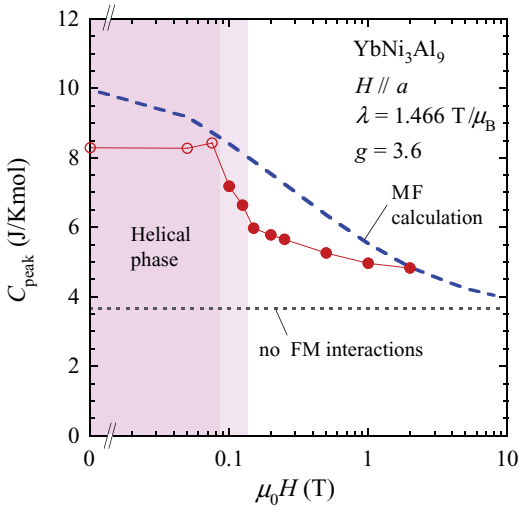

FIG. 7. (Color online) H dependence of the Schottky peak height C_{peak}. A mean-field model calculation is drawn with a dashed line. Note that the enhancement in C_{peak} (>3.65 J/K mol) is due to pronounced FM interactions.

results in the enhancement in C_{peak}. The parameter set λ and g have been determined so that the MF calculations reproduce reasonably well the Schottky peak position $T_p(H)$ in the H-T phase diagram and the value of magnetization. The best fit has been obtained with $\lambda = 1.466\ \mathrm{T}/\mu_B$ and $g = 3.6$, and the MF calculation of $T_p(H)$ is shown in Figs. 4(a) and 4(b).

In the H-T phase diagram of Fig. 4, the Schottky peak position is nicely reproduced by the calculated $T_p(H)$ in the PM phase. In the $H \to 0$ limit, the MF-calculated $T_p(H)$ provides a fictitious FM transition temperature $T_{FM} = 3.18$ K in zero field. The H dependence of C_{peak} shown in Fig. 7 is also qualitatively reproduced. In $YbNi_3Al_9$, however, the g value should depend on H to some extent, since the CEF excited levels mix gradually into the ground-state doublet due to the Zeeman effect. Deviations from the model calculation visible in Figs. 4 and 7 may be partly due to the simplification of the constant g. Another factor neglected in this model is the Kondo effect. According to the exact solution for the s-d impurity model,[19] C_{peak} is suppressed below 3.65 J/K mol in zero field and it increases gradually with increasing H, approaching 3.65 J/K mol for $g\mu_B H/k_B T_K \gg 1$. The slow decrease in C_{peak} in high fields shown in Fig. 7 might be due to combination of the Kondo effect and the FM interactions.

The helical magnetic ordering indicates the existence of mutually competing interlayer magnetic couplings. We use a simple model[20] which includes J_0 (>0), J_1 and J_2 representing exchange constants between magnetic moments in a FM Yb plane, with the adjacent Yb planes and with the next-nearest Yb planes, respectively. This model has an energy minimum solution with an HM structure with an interlayer magnetic moment turn angle ϕ ($\cos\phi = -J_1/4J_2$) given by

$$E_{ex} = -\bar{s}^2(J_0 + J_1\cos\phi + J_2\cos 2\phi). \qquad (2)$$

The propagation vector $\boldsymbol{q} = 0.8 \times \boldsymbol{c}^*$ determined by the neutron-scattering study[13] corresponds to $\phi = 96°$. Inserting this value into Eq. (2), the effective exchange integral for the HM phase is given by $J_{HM} \equiv J_0 - 2.43J_1$. In the field-induced FM phase ($\phi = 0°$), the effective exchange integral is given by $J_{FM} \equiv J_0 + 3.38J_1$. From $T_{HM} : T_{FM} = 3.41$ K: 3.18 K $= J_{HM} : J_{FM}$, the ratio $J_0 : J_1 : J_2 = 1 : -0.01 : -0.03$ is obtained. Significantly weak interlayer magnetic couplings, reflected in the 2 orders of magnitude smaller values of J_1 and J_2 than that of J_0, is consistent with the fact that Yb layers are largely separated; note that the strength of Ruderman-Kittel-Kasuya-Yosida (RKKY) interaction decays with the distance as $1/r^3$.

Normalized magnetoresistance $\rho(H)/\rho(0\ \mathrm{T})$ for $\boldsymbol{j} \parallel c$ and $H \parallel a$ (shown in Fig. 8) drops about 30% at H_M, which is in marked contrast with the absence of any signature in γ at the HM boundary. Based on this fact, we consider a simple two-carrier model, in which the Fermi sheets are separated into two parts FS_1 and FS_2. FS_1 disappears in the HM phase due to the nesting with the propagation vector $\boldsymbol{q}$. In the nonordered phase, it is expected that FS_1 plays a considerable role in the electric transport along the c axis, since it should have a rather flat surface perpendicular to the c axis.[21] FS_2 carries heavy quasiparticles contributing dominantly to the γ value. In the Drude picture, the contribution from FS_i to the electric conductivity can be expressed as $\sigma_i = n_i e^2\tau_i/m_i^*$, where n_i, τ_i, and m_i^* represent the carrier density, the relaxation time,

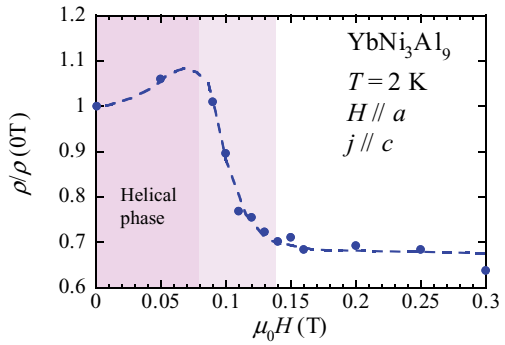

FIG. 8. (Color online) H dependence of normalized magnetoresistance $\rho(H)/\rho(0\ \mathrm{T})$. The dashed line is a guide to the eye.

and the effective mass of FS_i, respectively. From the 30% drop in $\rho(H)/\rho(0\ \mathrm{T})$ at H_M, $(n_2/m_2)/(n_1/m_1 + n_2/m_2) = 0.7$, tentatively assuming $\tau_1 = \tau_2$. Because γ does not show any noticeable increase at H_M within the experimental accuracy, $(n_1 m_1 + n_2 m_2)/n_2 m_2 \lesssim 1.02$. These two equations yield $m_2/m_1 \gtrsim 4.6$ and $n_2/n_1 \gtrsim 11$, indicating that the heavy quasiparticles are formed mainly on FS_2 not on FS_1. Note that if $\tau_1 < \tau_2$ is assumed, taking into account that FS_1 is a "hot sheet" associated with HM fluctuations, the lower bound value of m_2/m_1 becomes even larger. This anisotropic mass enhancement is consistent with recent dHvA measurements, in which the cyclotron effective masses of $m_c^*/m_0 = 3$–12 and 1–5 (m_0: the free electron mass) have been observed for $H \parallel c$ and $H \perp c$, respectively.[14] The present model is also consistent with the fact that $\rho(H)$ data for $\boldsymbol{j} \parallel a$ with $H \parallel b$ (not shown) does not show a noticeable jump at H_M, since FS_1 does not carry current along the a axis.

The realization of the helical magnetic ordering in $YbNi_3Al_9$ is caused by the weak but competing interlayer antiferromagnetic couplings ($J_1, J_2 < 0$). Such magnetic frustration may be able to cause quasiparticle mass enhancement, as discussed for LiV_2O_4[22] and for geometrically frustrated systems.[23] However, since the observed heavy quasiparticles do not reside in FS_1, which is responsible for the realization of the helical magnetic ordering, such a scenario is unlikely in $YbNi_3Al_9$.

The present findings suggest that the heavy quasiparticles are bound in the 2D Yb ferromagnetic layers (on part of FS_2). Heavy quasiparticles formed in ferromagnetic states have been reported so far in $CeRu_2Ge_2$ ($\gamma = 20\ \mathrm{mJ/K^2\ mol}$, ferromagnetic transition temperature $T_{FM} = 8$ K),[24] CeRuPO ($\gamma = 77\ \mathrm{mJ/K^2\ mol}$, $T_{FM} = 15$ K),[25] $CeAgSb_2$ ($\gamma = 65\ \mathrm{mJ/K^2\ mol}$, $T_{FM} = 9.6$ K),[26] $SmOs_4Sb_{12}$ ($\gamma = 820\ \mathrm{mJ/K^2\ mol}$, $T_{FM} = 3$ K),[27] UIr_2Zn_{20} ($\gamma = 450\ \mathrm{mJ/K^2\ mol}$, $T_{FM} = 2.1$ K),[28] UGe_2 ($\gamma = 35\ \mathrm{mJ/K^2\ mol}$, $T_{FM} = 52$ K, superconducting transition temperature $T_{SC} \sim 1$ K at 1.3 GPa),[29,30] URhGe ($\gamma = 164\ \mathrm{mJ/K^2\ mol}$, $T_{FM} = 9.5$ K, and $T_{SC} = 0.27$ K),[31,32] and UCoGe ($\gamma = 57\ \mathrm{mJ/K^2\ mol}$, $T_{FM} = 3$ K, $T_{SC} = 0.8$ K).[33] As the crystal structures of these compounds suggest, all of their electronic states have 3D characters. Even in such 3D systems, mechanisms of quasiparticle mass enhancement (or magnetic moment screening due to the Kondo effect) in FM states remain to be elucidated, not only experimentally but also theoretically.[34] To our knowledge, $YbNi_3Al_9$ is probably the first realization of the 2D version of such a system. We believe that $YbNi_3Al_9$ will provide an unparallel opportunity to investigate 2D heavy quasiparticles in FM layers.

ACKNOWLEDGMENTS

This work was supported by Grants-in-Aid for Scientific Research on Innovative Areas "Heavy Electrons" (20102007,A01-23102712) from MEXT and (C: 23540421) from JSPS.

*miyazaki-ryoichi@tmu.ac.jp
†aoki@tmu.ac.jp

[1] Y. Ōnuki, R. Settai, K. Sugiyama, T. Takeuchi, T. C. Kobayashi, Y. Haga, and E. Yamamoto, J. Phys. Soc. Jpn. **73**, 769 (2004).
[2] F. Steglich, P. Gegenwart, R. Helfrich, C. Langhammer, P. Hellmann, L. Donnevert, C. Geibel, M. Lang, G. Sparn, W. Assmus *et al.*, Z. Phys. B **103**, 235 (1997).
[3] J. Flouquet, D. Aoki, F. Bourdarot, F. Hardy, E. Hassinger, G. Knebel, T. D. Matsuda, C. Meingast, C. Paulsen, and V. Taufour, J. Phys.: Conf. Ser. **273**, 012001 (2011).
[4] H. Sato, H. Sugawara, Y. Aoki, and H. Harima, *Magnetic Properties of Filled Skutterudites*, Vol. 18 (Elsevier B.V., Amsterdam, 2009).
[5] H. Shishido, T. Shibauchi, K. Yasu, T. Kato, H. Kontani, T. Terashima, and Y. Matsuda, Science **327**, 980 (2010).
[6] Y. Mizukami, H. Shishido, T. Shibauchi, M. Shimozawa, S. Yasumoto, D. Watanabe, M. Yamashita, H. Ikeda, T. Terashima, H. Kontani *et al.*, Nat. Phys. **7**, 849 (2011).
[7] Y. Lutsyshyn, Y. Tokaychuk, V. Davydov, and R. Gladyshevskii, Chem. Met. Alloys **1**, 303 (2008).
[8] R. E. Gladyshevskii, K. Cenzual, H. D. Flack, and E. Parthé, Acta Cryst. **B49**, 468 (1993).
[9] Y. M. Kalychak, V. I. Zaremba, V. M. Baranyak, V. A. Bruskov, and P. Y. Zavalli, Russ. Metall. **1**, 213, (1989).
[10] C. Petrovic, P. G. Pagliuso, M. F. Hundley, R. Movshovich, J. L. Sarrao, J. D. Thompson, Z. Fisk, and P. Monthoux, J. Phys.: Cond. Matt. **13**, L337, (2001).
[11] T. Yamashita, R. Miyazaki, Y. Aoki, and S. Ohara, J. Phys. Soc. Jpn. **81**, 034705 (2012).
[12] S. Ohara, T. Yamashita, Y. Mori, and I. Sakamoto, J. Phys.: Conf. Ser. **273**, 012048 (2011).
[13] T. Hirayama, T. Tanaka, K. Munakata, T. Yamashita, S. Ohara, Y. Ohara, and Y. Uwatoko (private communication).
[14] S. Ohara, T. Yamashita, Y. Miura, R. Settai, Y. Onuki, and H. Harima (in preparation).
[15] P. H. Tobash, Y. Jiang, F. Ronning, C. H. Booth, J. D. Thompson, B. L. Scott, and E. D. Bauer, J. Phys.: Condens. Matter **23**, 086002 (2011).
[16] Note that the obtained value of γ depends on the functional form of C_{4f}. The data shown in Fig. 5 have been obtained with setting $\Delta = 0$. If Δ is included in the fitting parameter set, $\gamma = 140$ and 44 $\mathrm{mJ/K^2\ mol}$ for $\mu_0 H = 0$ and 5 T is obtained, respectively. Nevertheless, the overall behavior of γ vs H does not change

and no noticeable jump still appears at H_M. In $\mu_0 H \geqslant 4$ T, C_{4f} is strongly suppressed and the γT term dominates around 1 K, where C/T appears to be almost T independent, as shown in Fig. 2. Thereby, the γ value can be obtained more accurately as reflected in the smaller error bar. In $\mu_0 H = 5$ T, $\gamma_{Yb}/\gamma_{Lu} \sim 17$. This value is reasonable since the ratio of the dHvA cyclotron effective mass $m_c^*(\mathrm{Yb})/m_c^*(\mathrm{Lu}) = 3$–$25$ (depending on the branch) has been observed in this field region.[14]

[17] Y. Utsumi, H. Sato, S. Ohara, T. Yamashita, K. Kimura, S. Motonami, K. Shimada, S. Ueda, K. Kobayashi, H. Yamaoka *et al.*, Phys. Rev. B (to be published).

[18] This feature is in line with the fact that $YbNi_3Al_9$ does not show any noticeable quantum critical behaviors. In contrast, $YbAlB_4$ shows pronounced quantum critical behaviors and they are considered to be associated with the strong valence fluctuation of Yb ions. See S. Nakatsuji, K. Kuga, Y. Machida, T. Tayama, T. Sakakibara, Y. Karaki, H. Ishimoto, S. Yonezawa, Y. Maeno, E. Pearson *et al.*, Nat. Phys. **4**, 603 (2008), and Y. Matsumoto, S. Nakatsuji, K. Kuga, Y. Karaki, N. Horie, Y. Shimura, T. Sakakibara, A. H. Nevidomskyy, and P. Coleman, Science **332**, 316 (2011).

[19] K. Takegahara and T. Kasuya, Physica B **163**, 216 (1990).

[20] K. N. R. Taylor and M. I. Darby, *Physics of Rare Earth Solids* (Chapman and Hall, Ltd., London, 1972).

[21] Since 5 Al layers and 2 Ni layers are sandwiched between each Yb_2Al_3 layer along the c axis and the carriers on FS_1 have the Fermi velocity $\boldsymbol{v}_F \parallel c$, the carriers on FS_1 should have mainly Al-3p or Ni-3d characters. This feature explains the reason why m_1 is not much enhanced, as demonstrated in this model calculation.

[22] S. Burdin, D. R. Grempel, and A. Georges, Phys. Rev. Lett. **66**, 045111 (2002).

[23] P. Coleman and A. H. Nevidomskyy, J. Low Temp. Phys. **161**, 182 (2010).

[24] S. Süllow, M. C. Aronson, B. D. Rainford, and P. Haen, Phys. Rev. Lett. **82**, 2963 (1999).

[25] C. Krellner, N. S. Kini, E. M. Brüning, K. Koch, H. Rosner, M. Nicklas, M. Baenitz, and C. Geibel, Phys. Rev. B **76**, 104418 (2007).

[26] V. A. Sidorov, E. D. Bauer, N. A. Frederick, J. R. Jeffries, S. Nakatsuji, N. O. Moreno, J. D. Thompson, M. B. Maple, and Z. Fisk, Phys. Rev. B **67**, 224419 (2003).

[27] S. Sanada, Y. Aoki, H. Aoki, A. Tsuchiya, D. Kikuchi, H. Sugawara, and H. Sato, J. Phys. Soc. Jpn. **74**, 246 (2005).

[28] E. D. Bauer, A. D. Christianson, J. S. Gardner, V. A. Sidorov, J. D. Thompson, J. L. Sarrao, and M. F. Hundley, Phys. Rev. B **74**, 155118 (2006).

[29] Y. Onuki, I. Ukon, S. W. Yun, I. Umehara, K. Satoh, T. Fukuhara, H. Sato, S. Takayanagi, M. Shikama, and A. Ochiai, J. Phys. Soc. Jpn. **61**, 293 (1992).

[30] S. S. Saxena, P. Agarwal, K. Ahilan, F. M. Grosche, R. K. W. Haselwimmer, M. J. Steiner, E. Pugh, I. R. Walker, S. R. Julian, P. Monthoux *et al.*, Nature **406**, 587 (2000).

[31] I. H. Hagmusa, K. Prokeš, Y. Echizen, T. Takabatake, T. Fujita, J. C. P. Klaasse, E. Brück, V. Sechovský, and F. R. de Boer, Physica B **281**, 223 (2000).

[32] D. Aoki, A. Huxley, E. Ressouche, D. Braithwaite, J. Flouquet, J. P. Brison, E. Lhotel, and C. Paulsen, Nature **413**, 613 (2001).

[33] N. T. Huy, A. Gasparini, D. E. de Nijs, Y. Huang, J. C. P. Klaasse, T. Gortenmulder, A. de Visser, A. Hamann, T. Görlach, and H. V. Löhneysen, Phys. Rev. Lett. **99**, 067006 (2007).

[34] S. Yamamoto and Q. Si, Proc. Natl. Acad. Sci. USA **107**, 15704 (2010).